Conference paper
Griffo, Antonio, Wang, J. and Howe, D. (2008) *Stability analysis of electric power systems for 'more electric' aircraft.* In: 3rd International Conference "From Scientific Computing to Computational Engineering". 3rd IC-SCCE, 9 - 12 July 2008, Athens, Greece.

STABILITY ANALYSIS OF ELECTRIC POWER SYSTEMS FOR 'MORE ELECTRIC' AIRCRAFT

Antonio Griffo[1], Jiabin Wang[1], David Howe[1]

[1] Department of Electronic and Electrical Engineering
University of Sheffield
Mappin Street, S1 3JD Sheffield, UK
e-mail: a.griffo@sheffield.ac.uk, j.b.wang@sheffield.ac.uk

Keywords: Power systems, stability, linearization

Abstract. *This paper presents a comprehensive assessment of small-signal stability for a "more-electric" aircraft power system consisting of a synchronous variable-frequency generator which supplies several power electronic controlled loads via an 18-pulse autotransformer rectifier unit (ATRU) for AC-DC conversion. Functional models for key power system components and loads are derived. Numerical tools employed for the automatic calculation of linearized equations and operating points are described, and the influence of leading design and operational parameter on system stability is evaluated[*].*

1 INTRODUCTION

Future "more electric" aircraft power systems will be based on the interconnection of a wide range of components, resulting in a significantly more complex electrical distribution system with multiple distributed loads most of which are supplied and controlled by power electronic converters[1][2].

Negative impedance behaviour[3][4] resulting from constant power characteristic of tightly regulated power electronic loads can be a serious threat to system stability. The necessity to optimize system architecture, as well as the need to improve dynamic behaviour and avoid system instability requires a comprehensive understanding of the influence of design and control parameters and operating conditions on stability margins.

In general, time-domain simulation using detailed non-linear, time varying power system models, including system protection, control and operational limits, can be employed for accurate transient performance evaluation and stability assessment. This approach, however, is time consuming, requires vast computation resources and does not provide useful insights into the influence of the design, control, and operational parameters on the system dynamics and performance.

The application of computational efficient methods for assessing stability are made possible based on the fact that the majority of fast transient, time varying elements in a multiple-converter based power system are due to switching of power electronic devices, and the resulting switching harmonics will not have a significant influence on the system stability. By employing a state-space averaging technique, it is possible to derive an equivalent non-linear, time invariant system model and the small-signal stability of the power network under a given operating condition can be assessed either in frequency domain using Nyquist stability criteria[5]-[9] or by evaluating the eigenvalues of the linearised Jacobian matrix[10]-[11]. Industry application of these small signal stability analysis techniques is reliant on the establishment of a time-invariant state-space model which entails (i) derivation and validation of state-space averaging (SSA) models of power system components and subsystems, (ii) integration of SSA models to form a given power system architectures using an appropriate tool or simulation environment. The tool also has to be capable of computing the operating point for a given set of inputs and operating conditions, performing linearization and formulating the Jacobian matrix. Further, in order to perform the analysis efficiently, the entire process has to be executed automatically. At the present, however, validated state-space models suitable for stability assessment have not been extensively reported and no simulation tool that can perform the required procedures and operations is commercially available.

This paper presents a comprehensive small-signal stability assessment of the power system for "more-electric" aircraft consisting of a synchronous variable-frequency generator which supplies several power electronic loads connected via passive filters to a local high voltage dc bus, and employs an 18-pulse Autotransformer Rectifier Unit (ATRU) for AC-DC conversion. Numerical tools employed for the automatic calculation of linearized equations and operating points are described, and the influence of leading design and

---

operational parameter on system stability is evaluated.

2 DESCRIPTION OF MODELLING AND SIMULATION ENVIRONMENT

The high-voltage DC subsystem under consideration consists of five motor drive loads which are connected to a common ±270V DC bus via 4th order LC filters. The filters are used to attenuate harmonics so as to meet the power quality standard, and to provide a stabilizing effect for the motor drive loads which exhibit negative resistance behaviour. The DC bus is powered by an 18-pulse autotransformer rectifier unit (ATRU) whose AC inputs are directly connected to the output of a three-phase synchronous generator via feed cables. The AC bus voltage is regulated by the generator voltage controller at the point of regulation.

In order to provide a systematic and computationally efficient tool for stability assessment of "more electric" aircraft power systems, functional models for key power system components and loads have been developed and modelled using Modelica language[12]. Small-signal stability analyses, as well as time-domain simulations have been carried out in Dymola simulation environment. A library of components for stability analysis has been established as the outcome of on-going collaboration between the University of Sheffield and DLR.

2.1 Synchronous generator

A classical six-order model of the synchronous generator has been used[13]. In addition to the excitation winding, damper windings have been considered on both d- and q- rotor reference frame together with stator flux dynamics. The resulting differential-algebraic system of equations is given in eqs (1)-(4). The rotor voltage equations are:

$$
\begin{aligned}
\dot{\psi}_{fd} &= V_{fd} - R_{fd} I_{fd} \\
\dot{\psi}_{kD} &= -R_{kD} I_{kD} \\
\dot{\psi}_{kQ} &= -R_{kQ} I_{kQ}
\end{aligned}
\tag{1}
$$

where V_{fd} and I_{fd} are the exciter field voltage and current, R_{fd} is the field winding resistance, R_{kD} and R_{kQ} are equivalent d- and q-axis damper winding resistance, and ψ_{fd}, ψ_{kD} and ψ_{kQ} are the flux-linkages of the field winding and the d- and q-axis damper windings, respectively. The rotor flux-linkage equations are:

$$
\begin{aligned}
\psi_{fd} &= \left(L_{fd} + L_{md}\right)I_{fd} + L_{md}\left(-I_d + I_{kD}\right) \\
\psi_{kD} &= \left(L_{kD} + L_{md}\right)I_{kD} + L_{md}\left(-I_d + I_{fd}\right) \\
\psi_{kQ} &= \left(L_{kQ} + L_{mq}\right)I_{kQ} - L_{mq}I_q
\end{aligned}
\tag{2}
$$

where I_d and I_q are the d- and q-axis stator currents, I_{kD}, and I_{kQ} are the d- and q-axis rotor damper winding currents, L_{md} and L_{mq}, are the d- and q-axis magnetising inductances, and L_{kD} and L_{kQ} are the d- and q-axis leakage inductances of the rotor damper windings. The stator voltage equations are:

$$
\begin{aligned}
\dot{\psi}_d &= V_d + R_s I_d + \omega_s \psi_q \\
\dot{\psi}_q &= V_q + R_s I_q - \omega_s \psi_d
\end{aligned}
\tag{3}
$$

where, V_d and V_q are the d- and q-axis stator output voltages, R_s is the phase resistance of the stator winding, ψ_d, and ψ_q are the d- and q-axis flux-linkages of the stator winding, and ω_s is the synchronous angular frequency of the generator. The stator flux-linkage equations are:

$$
\begin{aligned}
\psi_d &= -\left(L_s + L_{md}\right)I_d + L_{md}\left(I_{fd} + I_{kD}\right) \\
\psi_q &= -\left(L_s + L_{mq}\right)I_q + L_{mq}I_{kQ}
\end{aligned}
\tag{4}
$$

where L_s is the leakage inductance of the stator winding. Fig. 1 shows the Dymola component model of the synchronous generator. The inputs are electrical angular frequency, and filed excitation voltage, and the outputs are d- and q-axis voltages and currents.
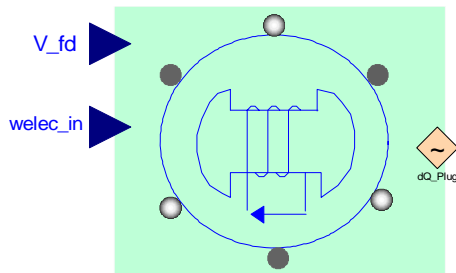
Figure 1 Synchronous generator model in Dymola library
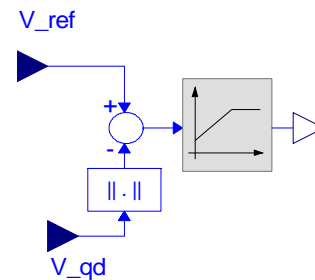
Figure 2 PI excitation control in Dymola library with anti-windup controller

2.2 PI excitation control

A PI controller with anti-windup limitation is assumed for the voltage regulation, as depicted in Fig. 1. Its parameters are derived by assuming the generator being represented as a simplified first order voltage behind transient reactance model[13] given in equation (5)

$$E_q^{'} = \frac{\omega_s L_{md}/R_{fd}}{T_{d0}^{'}} V_{fd} \tag{5}$$

where E'_q and T'_{d0} are the equivalent back emf and time constant of the model, respectively. This allows for specifying controller gains as a function of the required bandwidth ω_n and damping ratio ξ as follows.

$$
\begin{aligned}
K_p &= \frac{R_{fd}}{\omega_s L_{md}} \left(2\xi\omega_n T_{d0}^{'} - 1 \right) \\
K_i &= \frac{T_{d0}^{'} R_{fd}}{\omega_s L_{md}} \omega_n^2
\end{aligned}
\tag{6}
$$

2.3 18-pulse Autotransformer-Rectifier unit

Several different arrangements of 18-pulse autotransformer rectifiers have been proposed[14]-[15]. In this study the so-called direct symmetric ATRU topology has been adopted, whose Dymola model is depicted in Fig. 3. The ATRU consists of three six-pulse diode rectifiers, one of which is supplied by a three-phase voltage set in phase with the primary AC voltage, and the others by three-phase voltages displaced with respect to the AC input by 40 electrical degrees leading and lagging, respectively. Since at each time instant only one diode-bridge is conducting the positive current and one conducting the negative current, the three outputs are directly connected to the load without the need for interphase reactors. An analytical averaged valued model of the ATRU has been derived and validated by comparison with SABER simulation of the detailed ATRU model[17]. The developed analytical model is represented in Dymola as a library component, as shown in Fig. 3
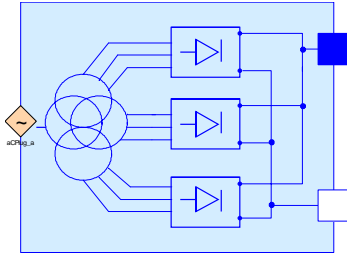
Figure 3 18-pulse ATRU in Dymola library
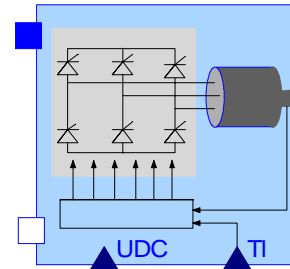
Figure 4 Motor drive load model in Dymola library

2.4 Motor drive load

If the DC voltage feedforward compensation is not employed, a motor drive load may deviate significantly from a constant power load, and its behaviour is influenced by the current and speed/position control bandwidths as well as operating conditions. A detailed Dymola motor drive load has been established as shown in Fig. 4. The model includes the dynamics of brushless permanent magnet drives in the d-q axis reference and an inner PI current control loop and an outer PI speed control loop[18]. This model provides a means to study the influence of the current and speed control loop bandwidths on the stability of the interconnected power system.

3. SMALL-SIGNAL STABILITY ANALYSIS OF HVDC NETWORK

Using the components established in the Dymola library described in section 2, the complete system of the HVDC network consisting of 5 power electronic controlled (motor-drive) loads fed by a variable frequency synchronous generator via the ATRU has been established, as shown in Fig. 5. Thanks to the powerful linearization capabilities of the Modelica language[12], it allows the small-signal stability analysis of the complete system to be carried out in an automatic manner. For the sake of simplicity, the power electronic controlled loads are represented as ideal constant power loads. For a given set of parameters and operating conditions the system contains 28 state-space variables. Small-signal stability analysis at a given operating point yields 28 eigenvalues
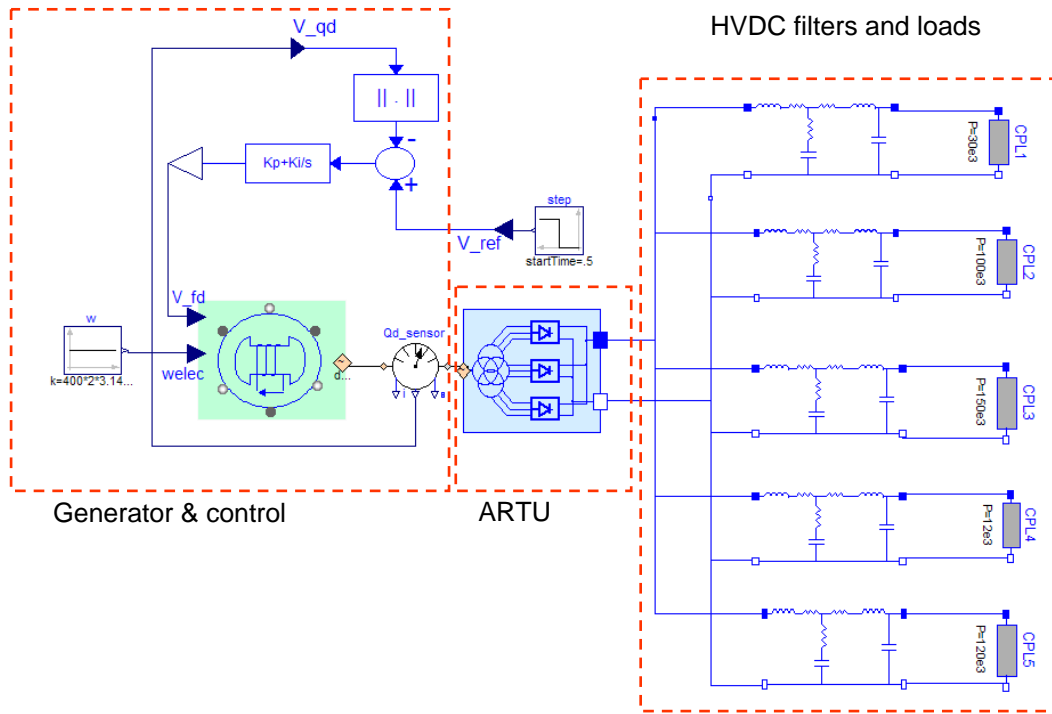
Figure 5 Dymola model of HVDC system

which are associated with the system components as follows:

- 4 for each filter-load combination
- 5 for synchronous generator
- 1 for voltage regulator
- 1 zero eigenvalue due to the angular reference
- 1 for ATRU

The system stability is dominated by five high frequency pairs of eigenvalues associated with each load, and one low frequency pair associated with the voltage regulator. Fig. 6 shows the eigenvalues loci as the generator operating frequency is varied from 200 to 800 Hz. For the sake of clarity only the modes with real part less than 500(1/s) are plotted. As can be seen, the increase in operating frequency decreases the damping of the ~1900 Hz modes which, according to modal analysis undertaken subsequently, are associated with filter-loads 3 and 5. The reduced stability margins that result from the increase in operating frequency can be explained as the effect of the decrease in steady-state DC bus voltage at the output of the rectifier as the operating frequency increases, as shown in Fig. 7. Because of the constant power nature of the loads, the decrease in steady-state DC bus voltage due to the so called reactive voltage drop results in an increase in steady-state DC bus current, as depicted in Fig. 8.
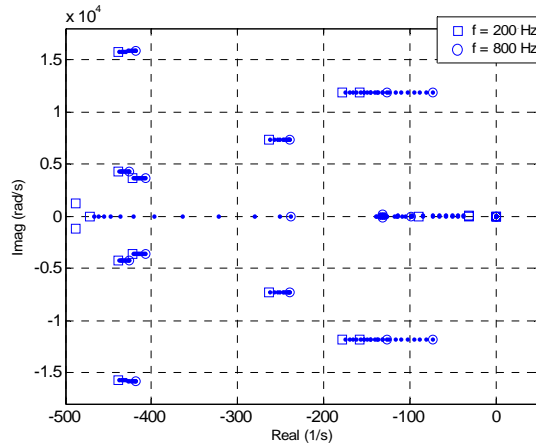
Figure 6 Influence of operating frequency on eigenvalue loci
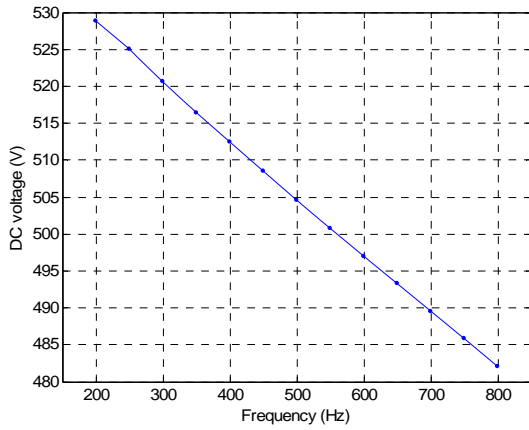
Figure 7 DC bus voltage vs. operating frequency
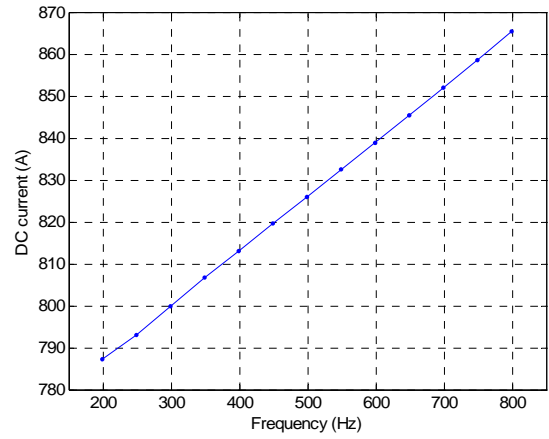
Figure 8 DC bus current vs. operating frequency

The combined effect of the decrease in DC bus voltage and the increase in DC bus current results in an increase in the equivalent resistance of the ATRU, as shown in Fig. 9, which models the reactive voltage drop, given by:

$$R_{eq} = \frac{V_{eq} - V_{DC}}{I_{DC}} \qquad (7)$$

The equivalent voltage, V_{eq}, is related to the magnitude of the AC phase voltage V_m by [16]:

$$V_{eq} = 2 \cdot \cos\frac{\pi}{18} \cdot V_m \cdot \frac{9}{\pi} \cdot 2\sin\frac{\pi}{18} \qquad (8)$$

Although the increase in the equivalent resistance should result in an improvement in stability margins, in this particular case, the destabilizing effect due to the reduction in DC voltage is more dominant.
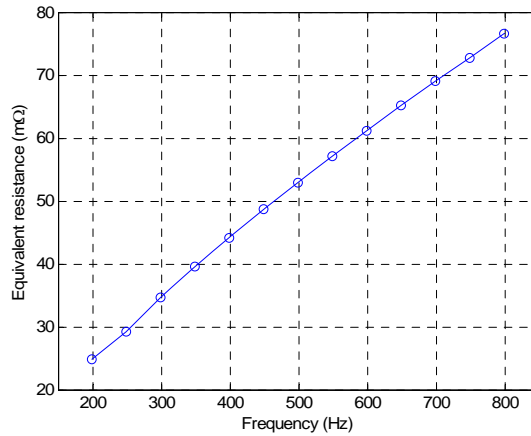
Figure 9 Equivalent resistance vs. operating frequency

Figure 10 shows the eigenvalues loci as the combined AC cable and transformer leakage inductance, which are assumed to be lumped together, is varied in the range 1µH-20µH. The increase of AC inductance has the effect of reducing the stability margins and the damping of the ~1900 Hz modes which become unstable when the leakage inductance L_{ac} is larger than 15 µH.

Finally, Fig. 11 shows the influence of AC voltage controller bandwidth and damping factor on the low frequency pair eigenvalues associated with the AC voltage regulator. Their influence on the other dominant pair eigenvalues is insignificant and therefore not shown.
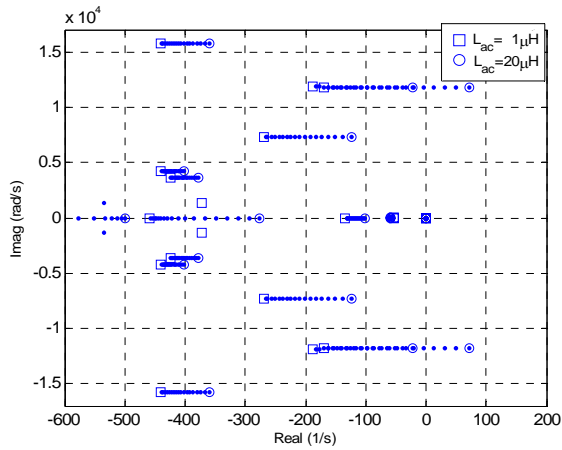
Figure 10 Influence of AC cable/Transformer leakage inductance on the root locus
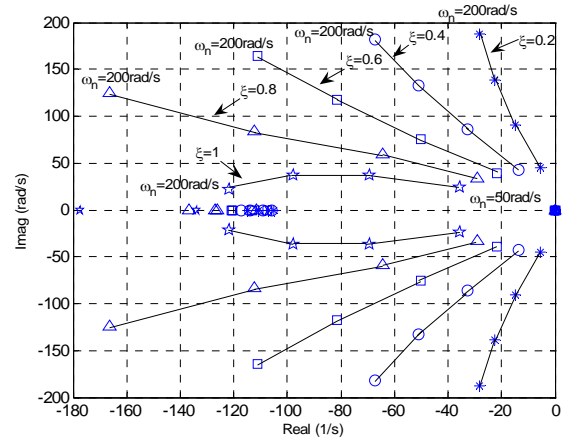
Figure 11 Influence of control parameters on the root locus

The modes associated with load voltages have been identified using selective modal analysis [18]-[19]. Table 1 lists the participation factors of the five load voltages with respect to each of their five modes.

Table 1 Participation factors of load voltages

	$\lambda_{5,6} =$ $-21617\pm j7137$	$\lambda_{13,14} =$ $-250\pm j7277$	$\lambda_{11,12} =$ $-131\pm j11801$	$\lambda_{15,16} =$ $-417\pm j3672$	$\lambda_{9,10} =$ $-162\pm j11828$
$|P(v_{CPL1},\lambda_i)|$	**1.86**	1.09e-3	0.28e-3	7.5e-6	0.15e-3
$|P(v_{CPL2},\lambda_i)|$	3.48e-4	**0.32**	4.21e-3	0.6e-4	2.2e-3
$|P(v_{CPL3},\lambda_i)|$	1.89e-5	5.38e-3	**0.62**	0.98e-3	0.28
$|P(v_{CPL4},\lambda_i)|$	9.49e-5	0.40e-3	1.2e-5	**0.49**	0.63e-5
$|P(v_{CPL5},\lambda_i)|$	1.91e-5	5.36e-3	0.28	0.97e-3	**0.61**

As is evident from the very low values of the off-diagonal participation factors, the coupling among different loads is negligible, except for the filter-loads 3 and 5, which show a certain degree of coupling due to the similar value of the loads and the equal values of filters' parameters.

The effect of the DC cable on the system stability can be investigated by using the lumped parameter model shown in Fig. 12.
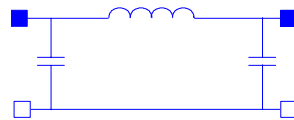
Figure 12 Lumped parameter model of DC cable

The equivalent capacitance and inductance can be determined according to the cable length and its characteristic parameters. The effect of the cable can be taken into account by inserting the equivalent circuit between the HVDC bus and the load filter in Fig. 5. It can be shown that as the cable length increases, the damping ratio of the eigenvalues associated with the load decreases, which implies a decrease in stability margin.

4. TIME DOMAIN SIMULATIONS

Time-domain simulations have been undertaken to validate the findings of the small signal stability analysis described in the previous sections. A step variation in the power demand from 140kW to 150kW at Load #3 has been applied at t = 0.5s, and the transient responses have been simulated. Figure 13 shows the resultant waveforms of the HVDC output voltage with two different values of the AC cable and transformer leakage inductances. As is evident, the system is stable when the AC cable and transformer leakage inductance is 15μH. However, instability of the system occurs when the AC cable and transformer leakage inductance is increased to

16μH. These results are consistent with those predicted by the small signal stability analyses, shown previously in Fig. 10. Simulations with different parameters and under different operating conditions have been performed and similar results have been observed.
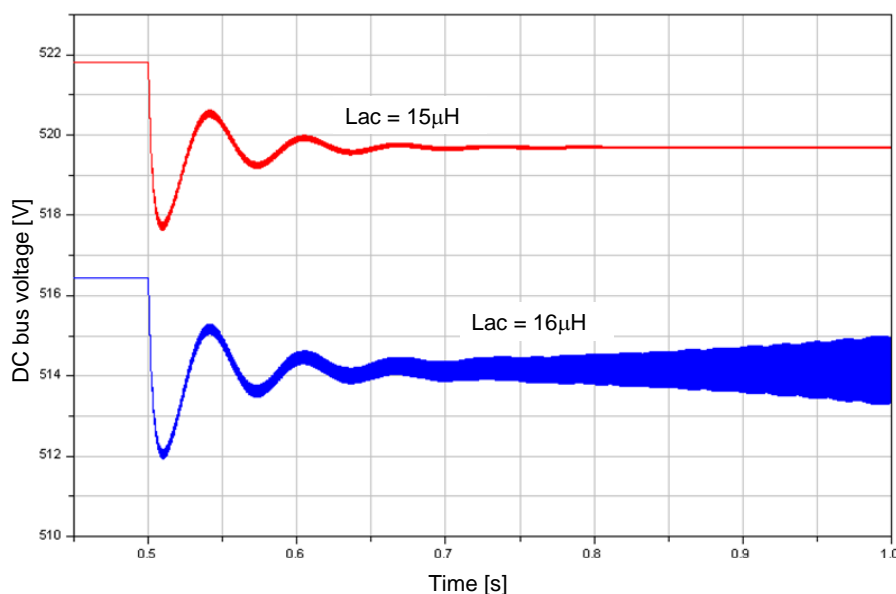
Fig. 13 DC bus voltage waveforms

5. CONCLUSIONS

Functional models for key power system components (Generator & control, ATRU, MCU, and filters, etc) suitable for stability analysis have been derived and a computational efficient tool in the Dymola simulation environment for small- and large-signal stability analysis has been established, and its utility demonstrated on a "more electric" aircraft power system comprising of a variable frequency AC generator, an 18-pulse ATRU and various power electronic controlled loads. Modal analysis has shown that the interaction between some loads is not significant. However system stability margin decreases as the generator operating frequency and AC leakage inductance increases. It has also been shown that the load filter parameters have crucial influence on the system stability. However, the influence of generator control on the system stability is limited.

ACKNOWLEDGEMENT

REFERENCES

[1]   A. Emadi and M. Ehsani, "Electrical system architecture for future aircraft", *Proc 34th Intersociety Energy Conversion Engineering Conferenc*e, British Columbia, Aug. 1999.
[2]   A. Emadi, B. Fahimi, and M. Ehsani, "On the concept of negative impedance instability in more electric aircraft power systems with constant power loads", *SAE Journal*, 1999-01-2545.
[3]   L. Han, J. Wang, and D. Howe, "Small signal stability studies of a 270V DC more electric aircraft power system", *Proc. IEE PEMD2006*, Dublin, pp. 197-201, 4-6 April, 2006.
[4]   A. Emadi, and M. Ehsani, "Negative impedance stabilising controls for PWM DC/DC converters using feedback linearization techniques", *Proc. IECECE2000*, pp. 613-620.
[5]   R. D. Middlebrook, "Input filter considerations in design and application of switching regulators", *Proceeding of IEEE Industrial Application Society Annual Meeting*, IAS76, 1976, pp. 366-382
[6]   S. S. Kelkar, and F. C. Lee, "Stability analysis of a buck regulator employing input filter compensation", *IEEE Trans. Aerospace Electronic Systems*, vol. 20, 1984, pp. 67-77

[7]   S. Sudoff, S. Glover, P. Lamm, D. Schmucker and D. Delisle, "Admittance space stability analysis of power electronics systems", *IEEE Trans. Aerospace and Electronic Systems*, vol. 36, 2000, pp. 965-973

[8]   C. M. Wildrick, F. C. Lee, B. H. Cho, and B. Choi, "Method of defining the load impedance specification for a stable distributed power systems", *IEEE Trans. Power Electronics*, vol. 10, 1995, pp. 280-285.

[9]   X. Feng, Z. Ye, K. Xing, F. C. Lee, and D. Borojevic, "Individual load impedance specification for a stable DC distributed power system", *Proceeding of IEEE Applied Power Electronics Conference*, vol. 2, 1999, 923-929.

[10] L. Han, J. Wang and D. Howe, "Small signal stability studies of 270V DC power system for more electric aircraft employing switched reluctance generator technology" *Proceedings of 25th International Council of the Aeronautical Sciences* (ICAS2006), Hamburg, Germany, 2006.

[11] L. Han, J. Wang, and D. Howe, "Stability assessment of distributed DC power systems for 'more electric' aircraft", *Proc. 4th IET International conference on Power Electronics, Machines and Drives*, York, UK, 2008, pp. 661-665.

[12] Dynasim AB, "Dymola User Mannaul Version 6", 2006.

[13] P. Kundur, "Power system stability and control", *McGraw Hill*, New York, 1994

[14] S. Choi, P. N. Enjeti and I. J. Pitel, "Polyphase transformer arrangements with reduced kVA capacities for harmonic current reduction in rectifier-type utility interface", *IEEE Trans. Power Electronics*, vol. 11, no. 5, Sept. 1996, pp.680-690.

[15] A. Uan-Zo-li, R. P. Burgos, H. Zhu, A. Roshan, F. Lacaux, F. Wang and D. Boroyevich, "Analysis of new 18-pulse direct symmetric autotransformer rectifiers with dual AC voltage feeding capability", *IECON* 2005, pp. 531-536.

[16] A. Griffo, J. Wang and D. Howe, "State-space average modelling of 18-pulse diode rectifier" submitted to ICSCCE2008.

[17] J. Wang, A. Griffo, L. Han, and D. Howe, "Input admittance characteristics of permanent-magnet brushless AC motor drive systems", *Proc. of 2007 IEEE Vehicle Power and Propulsion Conference* (VPPC2007), Arlington, USA, Paper ID, TS4-3, 2007.

[18] I. J. Perez-Arriaga, G. C. Verghese, F. C. Schweppe, "Selective modal analysis with applications to electric power systems, part 1: heuristic introduction", *IEEE Trans. Power Appar. and Sys*. Vol. PAS-101, no. 9, pp. 3117-3125. 1982

[19] I. J. Perez-Arriaga, G. C. Verghese, F. C. Schweppe, "Selective modal analysis with applications to electric power systems, part II: the dynamic stability problem", *IEEE Trans. Power Appar. and Sys*. Vol. PAS-101 no. 9, pp. 3126-3134. 1982